Title: An Interfacial Mechanism for Cloud Droplet Formation on Organic Aerosols

Authors: Christopher R. Ruehl,*[,1] James F. Davies and Kevin R. Wilson*

Affiliations: *Chemical Sciences Division, Lawrence Berkeley National Laboratory, Berkeley, CA 94720, USA*

[1] now at: *California Air Resources Board, Sacramento, CA 95814, USA*

* Correspondence to: chris.ruehl@arb.ca.gov, 916-323-1524 and krwilson@lbl.gov, 510-495-2474

Abstract: Accurate predictions of aerosol-cloud interactions require simple, physically accurate parameterizations of the cloud condensation nuclei (CCN) activity of aerosols. Current models assume that organic aerosol species contribute to CCN activity by lowering water activity. Here, droplet diameters at the point of CCN activation are measured for particles composed of dicarboxylic acids, or secondary organic aerosol, and ammonium sulfate. Droplet activation diameters are 40-60% larger than predicted if the organic is assumed to be dissolved within the bulk droplet, suggesting a new mechanism is needed to explain cloud droplet formation. A compressed film model explains how surface tension depression by interfacial organic molecules can alter the relationship between water vapor supersaturation and droplet size (i.e. the Köhler curve), leading to the larger diameters observed at activation.

One Sentence Summary: Direct measurements of droplet diameters formed on submicron organic aerosols under supersaturated water vapor conditions show that their activation to cloud droplets is controlled by interfacial organic films.

Main Text: Accurate predictions of the impact of aerosols on cloud properties, and thus the radiative balance of the atmosphere, rely on simple parameterizations of cloud droplet formation. Despite the simplicity required of such parameterizations, they must be based upon robust chemistry and physics to ensure the validity of climate predictions. From Köhler theory (*1*), the cloud condensation nuclei (CCN) activity of an aerosol is governed both by its size and its molecular constituents that can lower the water activity and/or surface tension of aqueous droplets below that of pure water. There are a number of extensively used empirical parameterizations of Köhler theory that neglect surface tension depression and assume cloud droplets form on particles that contain sufficient solute.(*2, 3*) Here, droplet sizes measured up to and including the point of cloud droplet activation reveal that most organic aerosols (OA) contribute to CCN by adsorbing to the air/droplet interface.

One popular parameterization of Köhler theory, known as κ-Köhler theory,(*3*) describes the lowering of water activity by a solute using a single parameter, κ; a dimensionless ratio of the molar volume of water to the average osmolar volume of the aerosol. κ-Köhler theory is used to interpret field observations and laboratory experiments in an effort to relate aerosol composition to hygroscopicity.(*4*) Although many field studies, including those in Colorado,(*5*) Ontario,(*6*) Coastal California,(*7*) and the Amazon(*8*), yield reasonable values of κ_{org} when interpreted via κ-Köhler theory, there are observations that suggest more complex behavior (non-ideal solution and surface tension effects) not captured in current water activity based parameterizations of CCN activity.(*9, 10*)

Neglecting surface activity in CCN parameterizations appears consistent with predictions of surface-bulk partitioning models (e.g. Szyszkowski-Langmuir adsorption theory). When using parameters obtained for macroscopic solutions, the bulk concentrations of surface-active solutes

are predicted to be strongly depleted in microscopic droplets, thus increasing water activity and negating any increase in CCN activity caused by a reduction in surface tension.(*11*) This has led many to conclude that accounting for surface activity is not necessary to accurately predict CCN activity of OA, despite measurements of reduced surface tension in macroscopic aqueous solutions of atmospheric OA and relevant model compounds.(*12, 13*) Furthermore, partitioning models fail to predict concentrations of surfactants in submicron droplets, suggesting significant limitations of current approaches to accurately describe surface activity at that length scale.(*14*)

Using a continuous flow streamwise thermal gradient chamber (see section S1 of (*15*)), we measure the diameter of droplets (D_{wet}) that form on mixed organic-ammonium sulfate (AS) particles at water vapor supersaturation (S, or RH – 100%) approaching and including the point of CCN activation. While it is common to compute Köhler curves to predict the critical supersaturation (S_c) of aerosols, direct measurements of D_{wet} as a function of S (*15*) allow OA CCN activity to be additionally constrained by droplet activation diameter ($D_{wet,c}$).

As shown in Fig. 1a, pure 200 nm diameter (D_{dry}) AS particles activate at $D_{wet,c} \sim 2.5$ μm, consistent with κ-Köhler theory. Mixed aerosols of AS and sucrose (known to be surface inactive) activate at $D_{wet,c} = 0.8$ μm, consistent with a water activity-based parameterization (Fig. 1b). These results are in contrast to AS aerosol coated with a series of small dicarboxylic acid (Figs. 1c and 1d, and Figs. S5-S7) and α-pinene secondary organic aerosol (SOA, Fig. 2). The functional form of D_{wet} vs. S deviates substantially from κ-Köhler predictions, with a $D_{wet,c}$ that is ~50% larger than predicted by constant κ_{org} for a given S_c. For succinic acid coated AS (Fig. 1d), $D_{wet,c}$ is observed to be 1.8 μm; substantially larger than predicted ($D_{wet,c} = 1.4$ μm) assuming $\kappa_{org} = 0.31$. A similar difference is observed for malonic acid (Fig. 1c). For SOA coated AS in Fig. 2, $D_{wet,c} = 1.3$-1.4 μm, much larger than the κ_{org} predictions of $D_{wet,c} = 0.9$ μm.

For pure AS aerosol, the evolution of D_{wet} with S, and the size of $D_{wet,c}$, are exactly what is predicted by κ-Köhler theory and serve to validate the experimental approach. The mixed AS/sucrose observations show that κ-Köhler theory correctly predicts D_{wet} vs. S and $D_{wet,c}$ for the case of a highly water soluble organic compound that does not depress surface tension (i.e. is surface inactive). In contrast AS aerosol coated with a series of dicarboxylic acids, some of which are known to be surface-active, exhibit much larger activation diameters and a different functional form of D_{wet} vs. S than is predicted by κ-Köhler theory (see Figs. 1 and 2, and S3-S7). While limited organic solubility can alter the shape of the Köhler curve,(*16*) it cannot explain the consistently large droplet activation diameters observed for these dicarboxylic acids, whose bulk solubility varies from near sucrose (i.e., malonic acid) to over two orders of magnitude smaller (see Table S1). The mixed SOA/AS aerosols exhibit the same deviation from κ-Köhler theory as the dicarboxylic acids. Collectively the observed differences between $D_{wet,c}$ for the organic acids (also SOA) and sucrose suggests that the discrepancies with κ-Köhler theory originate from surface effects rather than non-ideal behavior of mixtures.

To account for surface activity of organics within Köhler theory, an equation of state is required to relate the bulk and surface concentrations of the various solution components. Associated with the equation of state is an isotherm that relates organic surface concentration to surface tension. Previously, the Szyszkowsky-Langmuir equation(*13, 17*) was used to compute Köhler curves (i.e., to predict S_c) for model organic compounds.(*16*) This particular treatment of bulk-surface partitioning (section S2 of (*15*)) cannot fully explain the observed D_{wet} as a function of S. Instead, an equation of state that allows for a two-dimensional phase transition is required. To provide a self-consistent model description of the observations shown in Figs. 1-2, a compressed film model(*18*) is used to describe the relationship between surface tension depression

and organic surface coverage or thickness on the droplet (Figs. S3-S7). Model details can be found in section S2 of (*15*) and are described conceptually here. The model contains a 2D phase transition between "gaseous" and "compressed" surface states, which depends upon surface concentration (i.e. molecular packing). Since the quantity of organic material is fixed by the composition of the original dry aerosol, changes in surface tension occur when S increases and the droplet grows, decreasing the surface concentration by providing a larger surface area per molecule. At low S (below S_c), the surface organic concentration is high and the molecules adopt a compressed state, which lowers the droplet's surface tension below that of liquid water. At higher S (near S_c) the droplets are larger, the surface concentration is lower and the molecules at the interface are non-interacting (i.e. a gaseous surface state), with a droplet surface tension nearly equal to pure water. The data shown in Figs. 1 and 2 (and Fig. S3-S7) are best replicated if it is assumed that the surface tension increases linearly with decreasing surface concentration.(*18*) As shown in Figs. 1 and 2 (and Fig. S3-S7), the compressed film model can reasonably account for the functional form of S vs. D_{wet}. Although the compressed film model shows that some of the organic material is dissolved in the droplet bulk, the model reveals that for SOA and most of the model compounds (section S3 of (*15*)) the vast majority of the organic material is at the droplet surface (Fig. 2b and Figs. S3-S7), in stark contrast with the underlying assumption of κ-Köhler theory.

The compressed film model predicts that a particle will reach S_c when the surface film decreases in thickness to the point that individual molecules begin to separate - i.e., a 2-D phase transition occurs, and the surface tension no longer varies with increasing D_{wet}.(*15*) This occurs at a S and D_{wet} which lies on the post-activation portion of the Köhler curve for the bare inorganic AS seed. At this intersection point all of the hygroscopicity can be attributed to the reduction of water activity by AS. The compressed film model explains this by predicting that the organic

material is adsorbed to the interface (hence no decrease in water activity by the organic), but D_{wet} is large enough to lower the organic surface concentration to a point where the resulting surface tension is near that for pure water. Although there are several parameters needed to constrain the model, a single parameter approximation to the compressed film model can be used if it is assumed that all the organic material resides at the droplet surface. This parameter, termed δ_{org}, corresponds to a film thickness (in nm) on the droplet surface where the 2-D phase transition occurs (i.e., where the surface tension depression goes to zero). Although surface concentration is used more often than film thickness for monolayers of known composition, film thickness is preferable for discussions of particle hygroscopicity, since aerosol composition is often complex and poorly constrained molecularly, and because sizes (i.e., particle and droplet diameters) are measured in CCN experiments.

The S_c for a particle is computed from δ_{org} if both organic fraction (f_{org}) and κ_{inorg} (i.e., inorganic hygroscopicity) are known (see section S2 of (*15*)), which are the same set of parameters required to predict S_c given κ_{org}. In Fig. 3, the surface (δ_{org}) and bulk activity (κ_{org}) parametrizations are compared with additional measurements of S_c vs. dry organic coating thickness on AS seed particles for the same series of dicarboxylic acids and SOA. The measured critical supersaturation (S_c) decreases with increasing dry organic coating thickness for all particles measured. The data for each compound/SOA in Fig. 3 are fit with both a constant organic osmolar volume (related to κ_{org}) and film thickness (δ_{org}).

In most cases, constant κ_{org} does not replicate the observed curvature in S_c vs. coated diameter (Fig. 3), generally predicting a more shallow slope than is observed. There are two exceptions: malonic and suberic acid. However, the molar volumes required to replicate these data are much smaller than what is reported in the literature–malonic by 36%, and suberic by 3.7 times.

Such a dramatic increase in hygroscopicity cannot be explained by dissociation of these weak acids. In contrast, the δ_{org} approximation does capture the curvature observed in most plots of S_c vs. f_{org} observed in Fig. 3. Thus, the δ_{org} approximation to the compressed film model correctly accounts for both the droplet size at activation (Figs. 1-2, Fig. S3-S7) as well as the evolution of S_c with dry OA fraction (Fig. 3).

The compressed film model offers an explanation for some recent ambient CCN observations. In CCN closure studies, agreement between observations and predictions is often best when the organic aerosol fraction is assumed to be insoluble, as recently reported in California.(*19*) In particles that have similar amounts of organic and inorganic material, or are predominantly inorganic, there is not enough organic material to form a compressed film on the droplet at or near the point of activation. Although this organic material will be adsorbed to the droplet surface, there is an insufficient concentration at the interface to reduce surface tension; instead the organic will effectively behave as insoluble material with respect to CCN activation. Recently, activation diameters inferred from particle and droplet size distributions in urban fog were unexpectedly large,(*20*) similar to what is observed in this study. Finally, observations of enhanced organic aerosol hygroscopicity that were recently reported for a coastal site on Vancouver Island(*9*) do not seem reasonable for marine organic material, suggesting, in light of our results, a major contribution to CCN activity from surface activity could be likely.

The compressed film model also offers an explanation for some unresolved questions arising from laboratory CCN studies, including several single component OA that exhibit anomalously large CCN activity despite limited bulk solubility(*21-24*). For example, pimelic acid is CCN active ($\kappa = 0.14 - 0.16$), despite its low solubility that suggests κ_{org} should be 5 times smaller than observed.(*25*) This model predicts that most OA (especially OA of limited solubility)

is adsorbed to the surface of microscopic droplets. Thus the relatively small bulk concentrations may not, in fact, exceed solubility limits. Although Raoult (water activity) effects may also be important for aerosol with unknown or more complex composition (e.g. (*26*)), it is an unlikely explanation for the anomalously high CCN activity of individual compounds. The compressed film model also resolves the "gap" between κ_{org} values derived from CCN activity experiments, which are often much larger than those derived in subsaturated measurements of hygroscopic growth(*27*). The surface tension reduction by a compressed film will only increase hygroscopicity at high RH (i.e., near 100%)(*28*), while at lower RH, where the water activity term dominates, the effect of the film will be to lower hygroscopicity relative to the fully-soluble assumption.

These results point to an alternative mechanism for cloud droplet formation in mixed organic/inorganic aerosol. Although a water activity based parameterization correctly predicts the droplets sizes under supersaturated conditions for pure AS and sucrose (a non-surface active compound), it fails to correctly account for the larger cloud droplets that form on AS coated with a series of dicarboxylic acids (with a broad range of water solubility) and SOA. Thus it is unlikely that our results can be attributed to bulk solubility effects, but rather can be explained if most of the organic material exists as an interfacial compressed film, which reduces surface tension, allowing larger droplets to form prior to activation. At activation the compressed film transitions to a gaseous state and the surface tension of the droplet is nearly equal to pure water. Although the assumption that organic material dissolved in the droplet bulk may yield reasonable CCN predictions, in field measurements and in the laboratory, these results can help explain several outstanding questions and highlights the potential importance of interfacial organics in the formation of cloud droplets on organic aerosols.

References and Notes:

1. H. Kohler, The nucleus in and the growth of hygroscopic droplets. *Trans. Faraday Soc.* **32**, 1152-1161 (1936).
2. H. Abdul-Razzak, S. J. Ghan, A parameterization of aerosol activation 3. Sectional representation. *J. Geophys. Res.:Atmos.* **107**, AAC 1-1-AAC 1-6 (2002).
3. M. D. Petters, S. M. Kreidenweis, A single parameter representation of hygroscopic growth and cloud condensation nucleus activity. *Atmos. Chem. Phys.* **7**, 1961-1971 (2007).
4. J. L. Jimenez, M. R. Canagaratna, N. M. Donahue, A. S. H. Prevot, Q. Zhang, J. H. Kroll *et al.*, Evolution of organic aerosols in the atmosphere. *Science* **326**, 1525-1529 (2009).
5. E. J. T. Levin, A. J. Prenni, B. B. Palm, D. A. Day, P. Campuzano-Jost, P. M. Winkler *et al.*, Size-resolved aerosol composition and its link to hygroscopicity at a forested site in Colorado. *Atmos. Chem. Phys.* **14**, 2657-2667 (2014).
6. R. Y. W. Chang, J. G. Slowik, N. C. Shantz, A. Vlasenko, J. Liggio, S. J. Sjostedt *et al.*, The hygroscopicity parameter (κ) of ambient organic aerosol at a field site subject to biogenic and anthropogenic influences: relationship to degree of aerosol oxidation. *Atmos. Chem. Phys.* **10**, 5047-5064 (2010).
7. J. Wang, Y. N. Lee, P. H. Daum, J. Jayne, M. L. Alexander, Effects of aerosol organics on cloud condensation nucleus (CCN) concentration and first indirect aerosol effect. *Atmos. Chem. Phys.* **8**, 6325-6339 (2008).
8. S. S. Gunthe, S. M. King, D. Rose, Q. Chen, P. Roldin, D. K. Farmer *et al.*, Cloud condensation nuclei in pristine tropical rainforest air of Amazonia: size-resolved measurements and modeling of atmospheric aerosol composition and CCN activity. *Atmos. Chem. Phys.* **9**, 7551-7575 (2009).
9. J. D. Yakobi-Hancock, L. A. Ladino, A. K. Bertram, J. A. Huffman, K. Jones, W. R. Leaitch *et al.*, CCN activity of size-selected aerosol at a Pacific coastal location. *Atmos. Chem. Phys.* **14**, 12307-12317 (2014).
10. N. Good, D. O. Topping, J. D. Allan, M. Flynn, E. Fuentes, M. Irwin *et al.*, Consistency between parameterisations of aerosol hygroscopicity and CCN activity during the RHaMBLe discovery cruise. *Atmos. Chem. Phys.* **10**, 3189-3203 (2010).
11. R. Sorjamaa, B. Svenningsson, T. Raatikainen, S. Henning, M. Bilde, A. Laaksonen, The role of surfactants in Köhler theory reconsidered. *Atmos. Chem. Phys.* **4**, 2107-2117 (2004).
12. S. Ekström, B. Nozière, H. C. Hansson, The Cloud Condensation Nuclei (CCN) properties of 2-methyltetrols and C3-C6 polyols from osmolality and surface tension measurements. *Atmos. Chem. Phys.* **9**, 973-980 (2009).
13. M. C. Facchini, M. Mircea, S. Fuzzi, R. J. Charlson, Cloud albedo enhancement by surface-active organic solutes in growing droplets. *Nature* **401**, 257-259 (1999).
14. B. Nozière, C. Baduel, J.-L. Jaffrezo, The dynamic surface tension of atmospheric aerosol surfactants reveals new aspects of cloud activation. *Nat Commun* **5**, (2014).
15. Materials and methods and supporting analysis of the experimental data are available as supplementary materials on Science Online.
16. M. L. Shulman, M. C. Jacobson, R. J. Carlson, R. E. Synovec, T. E. Young, Dissolution behavior and surface tension effects of organic compounds in nucleating cloud droplets. *Geophys. Rev. Lett.* **23**, 277-280 (1996).

17. S. Henning, T. Rosenørn, B. D'Anna, A. A. Gola, B. Svenningsson, M. Bilde, Cloud droplet activation and surface tension of mixtures of slightly soluble organics and inorganic salt. *Atmos. Chem. Phys.* **5**, 575-582 (2005).
18. G. Jura, W. D. Harkins, Surfaces of solids .14. A unitary thermodynamic theory of the adsorption of vapors on solids and of insoluble films on liquid subphases. *J. Am. Chem. Soc.* **68**, 1941-1952 (1946).
19. R. H. Moore, K. Cerully, R. Bahreini, C. A. Brock, A. M. Middlebrook, A. Nenes, Hygroscopicity and composition of California CCN during summer 2010. *J. Geophys. Res.:Atmos.* **117**, (2012).
20. E. Hammer, M. Gysel, G. C. Roberts, T. Elias, J. Hofer, C. R. Hoyle *et al.*, Size-dependent particle activation properties in fog during the ParisFog 2012/13 field campaign. *Atmos. Chem. Phys.* **14**, 10517-10533 (2014).
21. K. Broekhuizen, P. P. Kumar, J. P. D. Abbatt, Partially soluble organics as cloud condensation nuclei: Role of trace soluble and surface active species. *Geophys. Rev. Lett.* **31**, (2004).
22. K. E. H. Hartz, J. E. Tischuk, M. N. Chan, C. K. Chan, N. M. Donahue, S. N. Pandis, Cloud condensation nuclei activation of limited solubility organic aerosol. *Atmos. Environ.* **40**, 605-617 (2006).
23. M. Hori, S. Ohta, N. Murao, S. Yamagata, Activation capability of water soluble organic substances as CCN. *J. Aerosol Sci.* **34**, 419-448 (2003).
24. A. Kristensson, T. Rosenorn, M. Bilde, Cloud Droplet Activation of Amino Acid Aerosol Particles. *J. Phys. Chem. A* **114**, 379-386 (2010).
25. M. Kuwata, W. Shao, R. Lebouteiller, S. T. Martin, Classifying organic materials by oxygen-to-carbon elemental ratio to predict the activation regime of Cloud Condensation Nuclei (CCN). *Atmos. Chem. Phys.* **13**, 5309-5324 (2013).
26. M. D. Petters, S. M. Kreidenweis, J. R. Snider, K. A. Koehler, Q. Wang, A. J. Prenni *et al.*, Cloud droplet activation of polymerized organic aerosol. *Tellus B* **58**, 196-205 (2006).
27. H. Wex, M. D. Petters, C. M. Carrico, E. Hallbauer, A. Massling, G. R. McMeeking *et al.*, Towards closing the gap between hygroscopic growth and activation for secondary organic aerosol: Part 1 – Evidence from measurements. *Atmos. Chem. Phys.* **9**, 3987-3997 (2009).
28. C. R. Ruehl, K. R. Wilson, Surface organic monolayers control the hygroscopic growth of submicrometer particles at high relative humidity. *J. Phys. Chem. A* **118**, 3952-3966 (2014).
29. G. C. Roberts, A. Nenes, A continuous-flow streamwise thermal-gradient CCN chamber for atmospheric measurements. *Aerosol Sci. Technol.* **39**, 206-221 (2005).
30. K. C. Young, A. J. Warren, A Reexamination of the Derivation of the Equilibrium Supersaturation Curve for Soluble Particles. *J. Atmos. Sci.* **49**, 1138-1143 (1992).
31. M. Kuwata, S. T. Martin, Phase of atmospheric secondary organic material affects its reactivity. *Proc Natl Acad Sci USA* **109**, 17354-17359 (2012).
32. D. Rose, S. S. Gunthe, E. Mikhailov, G. P. Frank, U. Dusek, M. O. Andreae *et al.*, Calibration and measurement uncertainties of a continuous-flow cloud condensation nuclei counter (DMT-CCNC): CCN activation of ammonium sulfate and sodium chloride aerosol particles in theory and experiment. *Atmos. Chem. Phys.* **8**, 1153-1179 (2008).

33. A. Zelenyuk, Y. Cai, D. Imre, From Agglomerates of Spheres to Irregularly Shaped Particles: Determination of Dynamic Shape Factors from Measurements of Mobility and Vacuum Aerodynamic Diameters. *Aerosol Sci. Technol.* **40**, 197-217 (2006).
34. N. L. Prisle, T. Raatikainen, A. Laaksonen, M. Bilde, Surfactants in cloud droplet activation: mixed organic-inorganic particles. *Atmos. Chem. Phys.* **10**, 5663–5683 (2010).
35. R. Sorjamaa, B. Svenningsson, T. Raatikainen, S. Henning, M. Bilde, A. Laaksonen, The role of surfactants in Köhler theory reconsidered. *Atmos. Chem. Phys.* **4**, 2107-2117 (2004).
36. K. Larsson, Alternation of melting points in homologous series of long-chain compounds. *J. Am. Oil Chem. Soc.* **43**, 559-562 (1966).
37. C. W. Harmon, C. R. Ruehl, C. D. Cappa, K. R. Wilson, A statistical description of the evolution of cloud condensation nuclei activity during the heterogeneous oxidation of squalane and bis(2-ethylhexyl) sebacate aerosol by hydroxyl radicals. *Phys. Chem. Chem. Phys.* **15**, 9679-9693 (2013).
38. K. C. Young, A. J. Warren, A Reexamination of the Derivation of the Equilibrium Supersaturation Curve for Soluble Particles. *J. Atmos. Sci.* **49**, 1138-1143 (1992).
39. P. P. Kumar, K. Broekhuizen, J. P. D. Abbatt, Organic acids as cloud condensation nuclei: Laboratory studies of highly soluble and insoluble species. *Atmos. Chem. Phys.* **3**, 509-520 (2003).
40. T. A. Rissman, V. Varutbangkul, J. D. Surratt, D. O. Topping, G. McFiggans, R. C. Flagan *et al.*, Cloud condensation nucleus (CCN) behavior of organic aerosol particles generated by atomization of water and methanol solutions. *Atmos. Chem. Phys.* **7**, 2949-2971 (2007).
41. M. Kuwata, W. Shao, R. Lebouteiller, S. T. Martin, Classifying organic materials by oxygen-to-carbon elemental ratio to predict the activation regime of cloud condensation nuclei (CCN). *Atmos. Chem. Phys. Discuss.* **12**, 31829-31870 (2012).
42. J. Y. Lee, L. M. Hildemann, Surface tensions of solutions containing dicarboxylic acid mixtures. *Atmos. Environ.* **89**, 260-267 (2014).

Acknowledgments: This work is supported by the Office of Science Early Career Research Program, through the Office of Energy Research, Office of Basic Energy Science of the U.S. Department of Energy under Contract No. DE-AC02-05CH11231. The CFSTGC-PDI was originally developed by Patrick Chuang and Anthanasios Nenes with support from the National Aeronautics and Space Administration's Atmospheric Radiation Measurement program.

SUPPLEMENTARY MATERIALS

www.sciencemag.org
Materials and Methods
Supplementary Text
Figs. S1 to S7
Tables S1-S3
References (32-43)

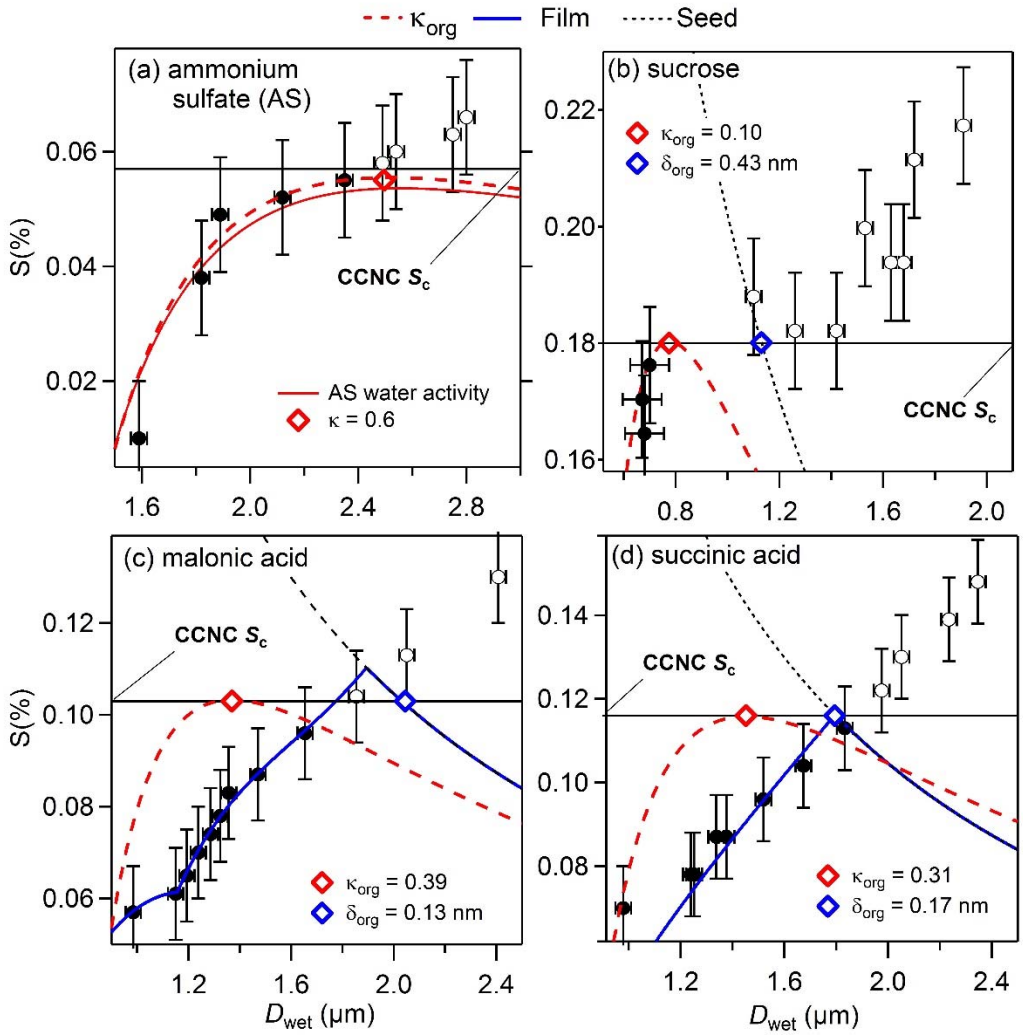

Figure 1: Köhler curve observations for **(a)** pure ammonium sulfate (AS), **(b)** sucrose + AS, **(c)** malonic acid + AS, and **(d)** succinic acid + AS particles. $D = 200$ nm for pure AS particles, and for all other particles $D = 150$ nm (50 nm AS seed + 50 nm radial coating thickness, corresponding to 89% organic by volume). As described in section S1 of (*15*), D_{wet}, is measured by Phase Doppler Interferometry, along the centerline of a thermal gradient chamber(*29*) after ~10 seconds of exposure to RH ~ 100% and is therefore not sensitive to decreases in surface tension that might occur over longer timescales as recently observed for aerosol and biological surfactants.(*14*) Solid and open circles represent unactivated and activated droplets, respectively. Since it is not always apparent when activation occurs solely from measurements of D_{wet}, the critical supersaturation (S_c) (horizontal solid black lines) is measured using a separate CCN counter (CCNC, Droplet Measurement Technologies). Dashed red lines are the Köhler curves predicted using a water activity parameterization (κ_{org}). Solid blue lines are those predicted by the compressed film model (see section S2 of (*15*)), and dashed black lines are those for the AS seed particles. The solid red line in panel (a) is the Köhler curve obtained with a parameterization of the water activity of dilute AS.(*30*) Also shown are the points of CCN activation predicted by κ_{org} (red diamonds) and δ_{org} (blue diamonds).

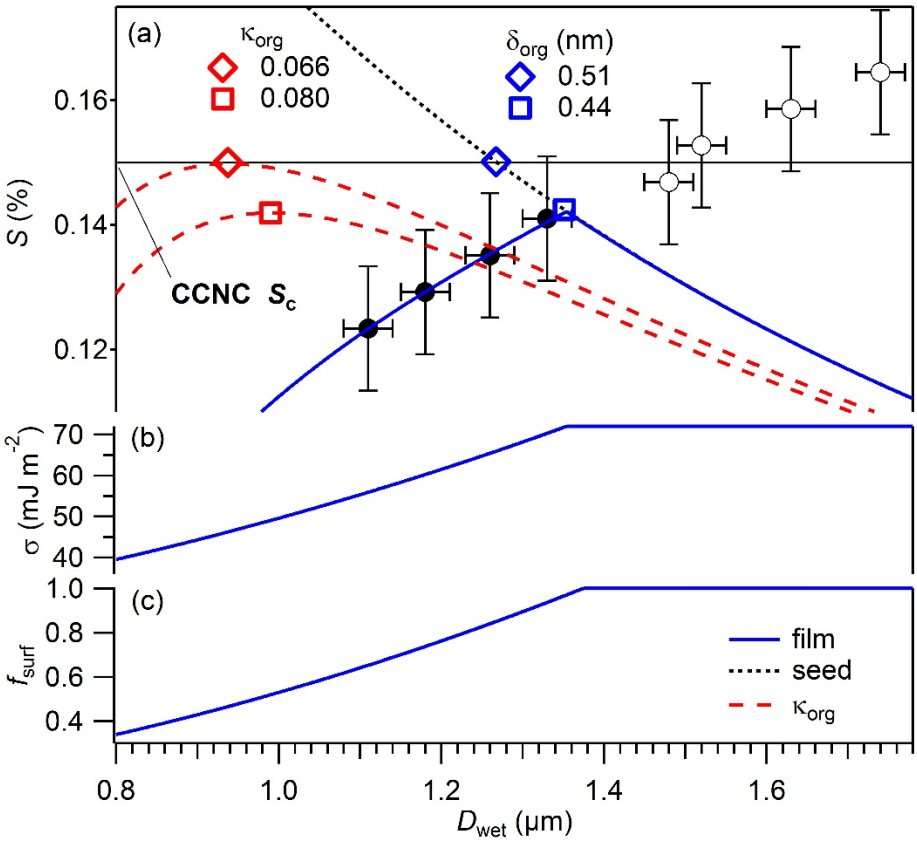

Figure 2: Köhler curve observations for AS + α-pinene SOA particles (D = 175 nm) prepared in a flow tube reactor. As described in section S1 of (*15*), SOA was generated by ozonolysis in a flow tube reactor and coated onto 85 nm diameter AS seeds (91% SOA by volume). **(a)** Dashed red lines are the Köhler curves predicted using a water activity parameterization; solid blue lines are those predicted with the compressed film model (details in section S2 of (*15*)), and dotted black lines are those for the AS seed particles. The horizontal black line indicates the critical supersaturation observed with a conventional CCN instrument (CCNC, Droplet Measurement Technologies). Also indicated is the point of CCN activation predicted by κ_{org} (red) and δ_{org} (blue) symbols. Included are the **(b)** surface tension (σ) and **(c)** fraction SOA at the surface (f_{surf}), as predicted by the compressed film model.

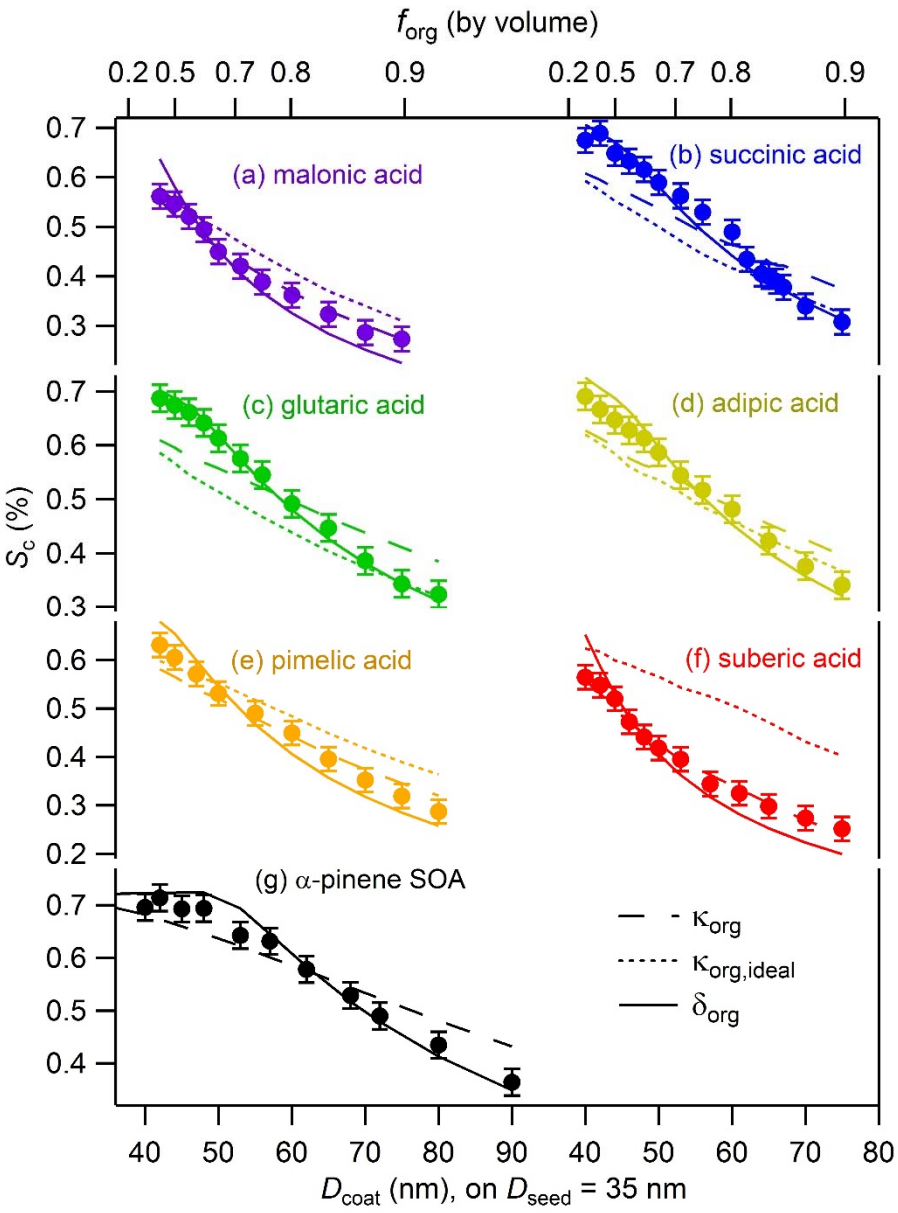

Figure 3: Critical supersaturation (S_c) as a function of coated dry diameter for (a-f) a series of dicarboxylic acids or (g) SOA generated via ozonolysis of α-pinene coated onto ammonium sulfate seed particles (D = 35 nm). Both seed and coated diameters are size-selected by differential mobility analyzer (TSI, Model 3080). Dashed and solid lines are best fits for each substance using a single parameter for organic hygroscopicity (κ_{org} and δ_{org}, respectively), and dotted lines indicate predictions assuming an ideal solution ($\kappa_{org,ideal}$). These values are listed in Table S1 of (*15*).